The Journal of Immunology

CXCR3 Mediates Renal Th1 and Th17 Immune Response in Murine Lupus Nephritis

Oliver M. Steinmetz, Jan-Eric Turner, Hans-Joachim Paust, Matthias Lindner, Anett Peters, Kirstin Heiss, Joachim Velden, Helmut Hopfer, Susanne Fehr, Thorsten Krieger, Catherine Meyer-Schwesinger, Tobias N. Meyer, Udo Helmchen, Hans-Willi Mittrücker, Rolf A. K. Stahl and Ulf Panzer

J Immunol 2009; 183:4693-4704; Prepublished online 4 September 2009;
doi: 10.4049/jimmunol.0802626
http://www.jimmunol.org/content/183/7/4693

The Journal of Immunology is published twice each month by
The American Association of Immunologists, Inc.,
1451 Rockville Pike, Suite 650, Rockville, MD 20852

Print ISSN: 0022-1767 Online ISSN: 1550-6606.

CXCR3 Mediates Renal Th1 and Th17 Immune Response in Murine Lupus Nephritis[1]

Oliver M. Steinmetz,[2]* Jan-Eric Turner,[2]* Hans-Joachim Paust,* Matthias Lindner,* Anett Peters,* Kirstin Heiss,† Joachim Velden,‡ Helmut Hopfer,§ Susanne Fehr,¶ Thorsten Krieger,† Catherine Meyer-Schwesinger,* Tobias N. Meyer,* Udo Helmchen,‡ Hans-Willi Mittrücker,† Rolf A. K. Stahl,* and Ulf Panzer[3]*

Infiltration of T cells into the kidney is a typical feature of human and experimental lupus nephritis that contributes to renal tissue injury. The chemokine receptor CXCR3 is highly expressed on Th1 cells and is supposed to be crucial for their trafficking into inflamed tissues. In this study, we explored the functional role of CXCR3 using the MRL/MpJ-*Fas*^{lpr} (MRL/*lpr*) mouse model of systemic lupus erythematosus that closely resembles the human disease. CXCR3$^{-/-}$ mice were generated and backcrossed into the MRL/*lpr* background. Analysis of 20-wk-old CXCR3$^{-/-}$ MRL/*lpr* mice showed amelioration of nephritis with reduced glomerular tissue damage and decreased albuminuria and T cell recruitment. Most importantly, not only the numbers of renal IFN-γ-producing Th1 cells, but also of IL-17-producing Th17 cells were significantly reduced. Unlike in inflamed kidneys, there was no reduction in the numbers of IFN-γ- or IL-17-producing T cells in spleens, lymph nodes, or the small intestine of MRL/*lpr* CXCR3$^{-/-}$ mice. This observation suggests impaired trafficking of effector T cells to injured target organs, rather than the inability of CXCR3$^{-/-}$ mice to mount efficient Th1 and Th17 immune responses. These findings show a crucial role for CXCR3 in the development of experimental lupus nephritis by directing pathogenic effector T cells into the kidney. For the first time, we demonstrate a beneficial effect of CXCR3 deficiency through attenuation of both the Th1 and the newly defined Th17 immune response. Our data therefore identify the chemokine receptor CXCR3 as a promising therapeutic target in lupus nephritis. ***The Journal of Immunology,*** **2009, 183: 4693–4704.**

Systemic lupus erythematosus (SLE)[4] is a chronic remitting and relapsing multisystem autoimmune disease that can affect the skin, joints, kidneys, lungs, nervous system, serous membranes, and/or other organs of the body (1). Renal involvement (lupus nephritis) is common in SLE and of central importance to the long-term prognosis (2). Typical morphological findings in human and experimental lupus nephritis are glomerular Ig deposits and the recruitment of mononuclear inflammatory cells. Infiltrating T cells, in particular, are thought to contribute to renal tissue damage in glomerular inflammation and, thus, to progressive loss of renal function (3). To date, diffuse and proliferative forms of glomerulonephritis, such as those found in SLE, have been believed to be predominantly Th1 cell mediated (4). However, the Th1 paradigm has recently been challenged by the identification of a new population of Th cells producing IL-17, which have been termed Th17 cells (5). Increasing evidence suggests that this newly identified T cell population is also crucial for the development and perpetuation of autoimmune disease (6–10). Two recent studies, including one by our own group, could show a role for Th17 cells in mouse models of glomerulonephritis (11, 12).

Before T cells can exert their detrimental effects on renal function in lupus nephritis, they have to reach the site of injury. The molecule families of chemokines and chemokine receptors are key regulators of directional leukocyte trafficking under homeostatic and inflammatory conditions (13, 14). By detecting chemokine concentration gradients via corresponding chemokine receptors, inflammatory cells are guided toward the focus of inflammation, where they exert their effector functions. Data from previous in vitro studies, experimental models, and studies in humans have highlighted the role of chemokines and their receptors in renal inflammation, including lupus nephritis (15–17). However, the functional importance of chemokine receptors in the recruitment of different T cell subsets into the kidney and the resulting clinical impact are still largely unknown. Chemokine receptors are expressed by effector T cells in a lineage-specific manner. Th1 cells express CXCR3, CCR5, and CXCR6, whereas Th2 cells express CCR3, CCR4, and CCR8 (18). Although CCR6 and CXCR3 have been detected on Th17 cells (19–21), the chemokine receptor expression profile of Th17 cells has yet to be fully elucidated, particularly with respect to a direct functional response.

Our group previously generated CXCR3-deficient mice and demonstrated that CXCR3$^{-/-}$ animals were partly protected from immunologically mediated injury by a reduction in renal T cell trafficking in a model of acute glomerulonephritis (22). However, this model of glomerulonephritis is an acutely induced "one-hit"

*III. Medizinische Klinik, †Institut für Immunologie, and ‡Institut für Pathologie, Universitätsklinikum Hamburg-Eppendorf, Hamburg, Germany; §Institut für Pathologie, Universitätsspital Basel, Basel, Switzerland; and ¶Servicegruppe Morphologie, Zentrum für Molekulare Neurobiologie Hamburg, Hamburg, Germany

Received for publication August 13, 2008. Accepted for publication July 31, 2009.

The costs of publication of this article were defrayed in part by the payment of page charges. This article must therefore be hereby marked *advertisement* in accordance with 18 U.S.C. Section 1734 solely to indicate this fact.

[1] This work was supported by grants from the Deutsche Forschungsgemeinschaft (PA 754/6-3, STE 1822/1-1, and KFO 228 Project 1).

[2] O.M.S. and J.-E.T. contributed equally to this work.

[3] Address correspondence and reprint requests to Dr. Ulf Panzer, Universitätsklinikum Hamburg-Eppendorf, III. Medizinische Klinik, Martinistrasse 52, 20246 Hamburg, Germany. E-mail address: panzer@uke.uni-hamburg.de

[4] Abbreviations used in this paper: SLE, systemic lupus erythematosus; BUN, blood urea nitrogen; DN, double negative; IP10, IFN-γ-inducible protein 10; Mig, monokine induced by IFN-γ; NTN, nephrotoxic serum nephritis; PAS, periodic acid-Schiff; SNP, single nucleotide polymorphism; ITAC, IFN-inducible T cell α chemoattractant.

www.jimmunol.org/cgi/doi/10.4049/jimmunol.0802626

model that involves an inflammatory response with a certain time course. In contrast, many human autoimmune diseases such as lupus nephritis develop over a long time and are caused by multiple and chronic inflammatory stimuli.

The function of CXCR3 in lupus nephritis has not yet been determined. This study was therefore performed to define the role of CXCR3 in MRL/MpJ-*Fas*^{lpr} (MRL/*lpr*) mice, a well-established mouse model of human lupus nephritis. CXCR3$^{-/-}$ mice were backcrossed into the MRL/*lpr* background to address two major issues, as follows: 1) What is the potential impact of CXCR3 deficiency on the clinical course of MRL/*lpr* nephritis? 2) What is the effect on renal Th1 and Th17 immune responses?

Materials and Methods

Animals

MRL/MpJ-*Fas*^{lpr} (MRL/*lpr*) and MRL/MpJ (MRL) mice were purchased in 2003 from The Jackson Laboratory and subsequently maintained as breeding colonies in our animal facility. CXCR3$^{-/-}$ C57BL/6 mice were generated as published by us (22). The CXCR3 gene is located on the X chromosome. Male mice hemizygous for the CXCR3 mutation are CXCR3 deficient, and are therefore referred to as CXCR3$^{-/-}$. All mice were housed under specific pathogen-free conditions. CXCR3$^{-/-}$ mice were backcrossed for at least eight generations into the MRL/*lpr* background to obtain CXCR3$^{-/-}$ MRL/*lpr* animals. To minimize genetic background differences between the animals, the CXCR3 wild-type MRL/*lpr* mice used in this study were derived from the same litter as the CXCR3$^{-/-}$ MRL/*lpr* animals. MRL mice were used as healthy controls. Only male animals were used for the experiments. Animal experiments were performed according to national and institutional animal care and ethical guidelines, and had been approved by local committees.

Patients and tissue samples

Renal biopsy samples were obtained from the archive of the Department of Pathology of the University Hospital of Hamburg-Eppendorf. Only patients in whom lupus nephritis of World Health Organization types III and IV had been diagnosed in our center were included in the study. Specimens of the control group derived from patients without autoimmune kidney diseases. The study was conducted with approval from the local ethics committee.

Genotyping

All mice were genotyped by PCR using genomic DNA that was prepared from tail biopsies. The following primers were used: CXC-EX2-F$_1$, 5′-TGT CCT CCT TGT AGT TGG GCT-3′; CXC-UTR-R1, 5′-TTG GCC TGA GCT GCT GGG AT-3′; and Neo5′-R, 5′-CTA AAG CGC ATG CTC CAG ACT GCC-3′ (for genotyping of the CXCR3 locus); Fas forward, 5′-AAAGGTTACAAAAGGTCACCC-3′; Fas reverse, 5′-GGTGCAG CCAGAAGCTAG-3′; and *lpr* reverse, 5′-GTTCCTCTTAGCATCTCTC TGC-3′ (for genotyping of the *fas* mutation).

Additionally, a genome-wide screening with 201 autosomal single nucleotide polymorphism (SNP) markers, including the H-2 locus, as well as 16 SNP markers on the X chromosome, was conducted by the JAX Genome Scanning Service at The Jackson Laboratory.

Functional studies

For urine collection, mice were housed in metabolic cages for 6 h one day before sacrifice. Urinary albuminuria was determined by standard ELISA analysis (mice-albumin kit; Bethyl Laboratories). At the time of sacrifice, blood was drawn for blood urea nitrogen (BUN) measurement.

Real-time RT-PCR analysis

Total renal RNA from the cortex of frozen murine kidneys was prepared, as described previously (23). RNA from archived formalin-fixed and paraffin-embedded human biopsy specimens was extracted from two 10-μm-thick sections of each patient. The High Pure FFPE RNA kit (Roche) was used as published (23). Biopsy specimens from the same patients were used for immunohistochemistry. Real-time PCR was performed for 40 cycles (initial denaturation, 95°C, 10 min; denaturation, 15 s, 95°C; primer annealing and elongation, 1 min, 60°C) with 1.5 μl of cDNA samples in the presence of 2.5 μl (0.9 μM) of specific murine and human primers (primer sequences are available upon request) and 12.5 μl of 2× Platinum SYBR Green qPCR Supermix (Invitrogen) using an AbiPrism Sequence Detection System 7000 (Applied Biosystems). To account for small RNA and cDNA variability, an 18S rRNA PCR was run in parallel. All samples were run in duplicate and normalized to 18S rRNA, as described recently (24).

In situ hybridization

In situ hybridization procedures were performed, as described previously (24). In brief, probes for monokine induced by IFN-γ (Mig)/CXCL9, IFN-γ-inducible protein 10 (IP10)/CXCL10, IFN-inducible T cell α chemoattractant (ITAC)/CXCL11, and CXCR3 used for in situ hybridization were prepared by in vitro transcription of subcloned cDNA with incorporation of ^{35}S-labeled UTP. The 326-bp Mig/CXCL9 probe corresponds to nt 18–344 of sequence M34815, the 290-bp IP10/CXCL10 probe corresponds to nt 264–554 of sequence NM_021274, the 235-bp ITAC/CXCL11 probe corresponds to nt 56–291 of sequence NM_019494, and the 286-bp CXCR3 probe corresponds to nt 1139–1425 of sequence NM_009910 (GenBank accession numbers http://www.ncbi.nlm.nih.gov/GenBank/).

Morphological examinations

Light microscopy was performed by routine procedures, as described previously (23). The percentage of glomeruli with crescents and capillary necrosis was assessed by a nephropathologist in at least 70 glomeruli per mouse in a blinded fashion using periodic acid-Schiff (PAS)-stained paraffin sections. For electron microscopy, kidney tissue was fixed in 4% paraformaldehyde in 0.1 M cacodylate buffer, embedded in araldite, cut with an Ultracut E ultramicrotome (Reichert Jung), and stained with uranyl acetate and lead citrate. Specimens were examined with a Zeiss EM 109 electron microscope, as previously described (22).

Immunohistochemistry

Paraffin-embedded sections (2 μm) were stained with the following Abs directed against the T cell marker CD3 (A0452; DakoCytomation): the monocyte-specific marker F4/80 (BM8; BMA); a marker for glomerular monocytes MAC-2 (M3/38; Cedarlane Laboratories); C3 (Cappel Laboratories; Organon Teknika); and mouse IgG, IgG1, IgG2a, IgG2b, or IgG3 (all Jackson ImmunoResearch Laboratories). Tissue sections were developed with the Vectastain ABC-AP kit (Vector Laboratories). Using light microscopy, F4/80-, MAC-2-, and CD3-positive cells were counted in a blinded fashion in 50 glomerular cross-sections and 30 tubulointerstitial high power fields per kidney.

For simultaneous visualization of CD3$^+$ T cells, CD19$^+$ B cells, and CD11b$^+$ macrophages, 10 μm frozen sections of mouse spleen, thymus, and lymph nodes were fixed in −20°C acetone for 5 min and air dried. Unspecific binding was blocked with 5% normal horse serum (Vector Laboratories) for 30 min at room temperature. Sections were incubated overnight with rabbit anti-CD3 (DakoCytomation) and FITC-conjugated rat anti-CD19 (Miltenyi Biotec) at 4°C. After washing, incubation with Cy5-conjugated anti-rabbit (DakoCytomation) and biotinylated anti-rat (DakoCytomation) was performed for 30 min, followed by incubation with PE-conjugated rat anti-CD11b (Miltenyi Biotec) and avidin-FITC (Vector Laboratories). Sections were mounted with Fluoromount-G (Southern Biotechnology Associates) and analyzed with an LSM 510 Beta microscope (Zeiss) using the LSM software.

For human studies, paraffin tissue sections of renal biopsy specimens (2 μm) were placed in citrate buffer (pH 6.1) and heated in the microwave for 25 min. For single staining, tissue was then incubated with anti-human CXCR3 mAb (1C6; BD Pharmingen) or monoclonal anti-human CD4 (MT310; DakoCytomation). Tissue sections were developed with the Vectastain ABC-AP kit (Elite Kit, Vectastain PK-6102; Vector Laboratories), as described (25). For double staining, renal tissue was incubated with rabbit anti-human CD4 (SP35; Biozol) and mouse CXCR3 (1C6; BD Pharmingen) Abs. Secondary Abs used were Alexa Fluor 488 donkey anti-mouse (A-21202; Molecular Probes/Invitrogen) and Cy3 donkey anti-rabbit (711-165-152; Jackson ImmunoResearch Laboratories/Dianova). Analysis was conducted using the LSM 510 Beta microscope (Zeiss).

Isolation of leukocytes from renal, lymphatic, and intestinal tissues

Previously described methods were used for renal cell isolation from murine kidneys (26). In brief, kidneys were finely minced and digested for 45 min at 37°C with 0.4 mg/ml collagenase D (Roche) and 0.01 mg/ml DNase I in DMEM (Roche) supplemented with 10% heat-inactivated FCS. Cell suspensions were sequentially filtered through 70- and 40-μm nylon meshes and washed with HBSS without Ca^{2+} and Mg^{2+}. Single-cell suspensions were separated using Percoll density gradient (70 and 40%) centrifugation (27). The leukocyte-enriched cell suspension was aspirated from the Percoll interface. For single-cell suspension of spleens and lymph

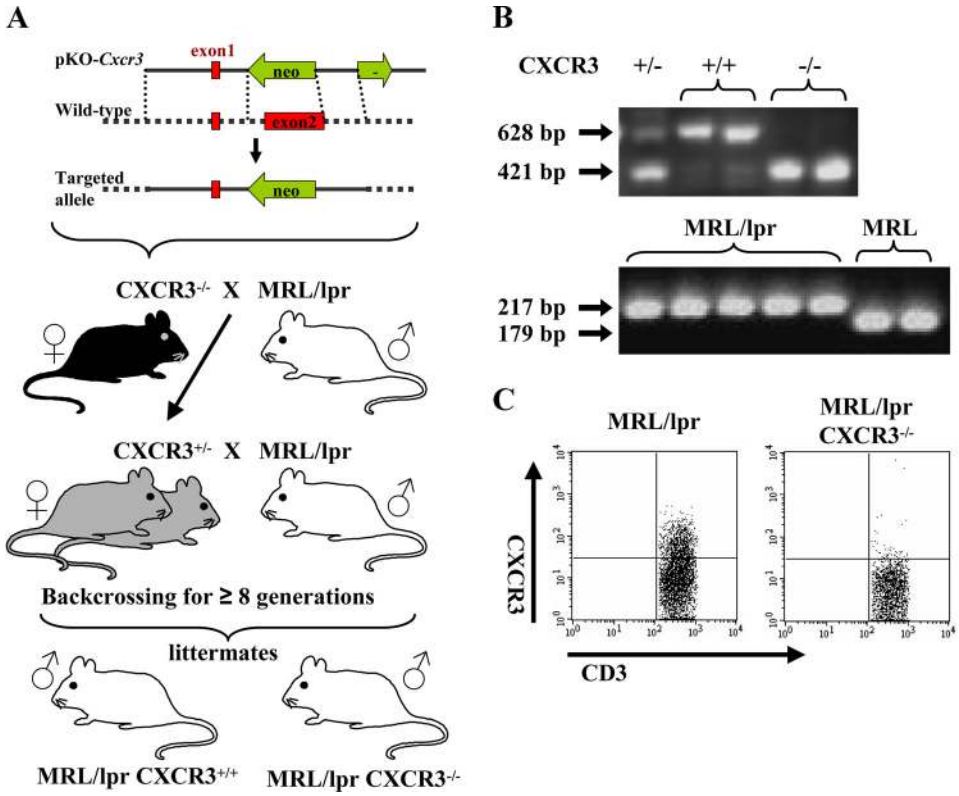

FIGURE 1. Generation and characterization of MRL/*lpr* CXCR3$^{-/-}$ mice. *A*, Introduction of the targeting vector pKO-CXCR3 resulted in a complete knockout of exon 2 of the X chromosomal CXCR3 gene. Female F_1 CXCR3$^{-/-}$ mice were crossed with male MRL/*lpr* animals. CXCR3 heterozygous female offspring were then backcrossed with MRL/*lpr* mice for at least eight generations, which resulted in male MRL/*lpr* CXCR3$^{-/-}$ and MRL/*lpr* CXCR3 wild-type littermates. *B*, PCR screening for the CXCR3 mutation resulted in a band at 628 bp in wild-type animals, at 421 bp in CXCR3$^{-/-}$ animals, and in both bands in heterozygous mice. Screening for the *fas* mutation resulted in a band at 179 bp in MRL control animals and at 217 bp in MRL/*lpr* mice. *C*, FACS analysis showed absence of CXCR3 on CD3$^+$ splenocytes from MRL/*lpr* CXCR3$^{-/-}$ mice.

nodes, organs were minced and sequentially passed through 70- and 40-μm nylon meshes. After lysis of erythrocytes with ammonium chloride, cells were washed several times with HBSS (without Ca^{2+} and Mg^{2+}) and resuspended in RPMI 1640 with 10% FCS. Cell viability was assessed by trypan blue staining.

Intraepithelial lymphocytes and lamina propria lymphocytes were isolated, as previously described (28). Briefly, after the excision of Peyer's plaques, small intestines of the individual mice were cut open and washed twice in PBS. Small intestines were stirred at 37°C for 20 min in complete RPMI 1640 medium, and then washed twice by shaking in complete RPMI 1640 medium for 0.5 min. Supernatants were filtered through a 70-μm nylon sieve, and lymphocytes were enriched using Percoll density gradient (70 and 40%) centrifugation. After intraepithelial lymphocyte isolation, the small intestine was cut into 5-mm pieces and digested for 60 min at 37°C in RPMI 1640 with 10% FCS supplemented with collagenase D (Roche) and collagenase type VIII (Sigma-Aldrich). Resulting cell suspensions were filtered through a 70-μm nylon sieve and centrifuged to pellet the cells. Cells were washed in RPMI 1640 with 10% FCS and further purified by a 70/40% Percoll density gradient.

Flow cytometry

To analyze the H-2 haplotype, peripheral blood was obtained from CXCR3 wild-type MRL/*lpr*, CXCR3$^{-/-}$ MRL/*lpr*, and C57BL/6 mice. Leukocytes were then stained for CD45-PerCP in combination with either H-2 K^b-FITC, H-2 K^k-PE, H-2 I-A^b-FITC, H-2 I-A^k-PE, or H-2 I-E^k-PE (all BD Pharmingen), and subsequently analyzed by FACS.

For leukocyte differentiation, isolated cells were stained with fluorochrome-labeled Abs specific for CD3 (allophycocyanin; 17A2, R&D Systems, or Pacific blue, eBio500A2 eBioscience), CD4 (PE; GK1.5, Miltenyi Biotec, or allophycocyanin-Alexa Fluor 750, eBioscience), CD8 (PerCP; BD Pharmingen), and CXCR3 (allophycocyanin; CXCR3-173; eBioscience) for 25 min at 4°C. Before Ab incubation, unspecific staining was blocked with normal mouse serum. Staining of intracellular IFN-γ and IL-17 was performed, as recently described (29). In brief, isolated leukocytes were activated by incubation at 37°C, 5% CO_2, for 5 h with PMA (5 ng/ml; Sigma-Aldrich) and ionomycin (1 μg/ml; Calbiochem-Merck) in RPMI 1640 with 10% FCS. After 30 min of incubation, brefeldin A (10 μg/ml; Sigma-Aldrich) was added. After several washing steps and staining of cell surface markers, cells were incubated with Cytofix/Cytoperm (BD Biosciences) at 4°C for 20 min to permeabilize cell membranes. Then, intracellular IL-17 and IFN-γ were stained using rat anti-mouse IL-17A Ab (PE; TC11-18H10; BD Pharmingen) and an anti-IFN-γ Ab (FITC; XMG1.2; BD Pharmingen). Experiments were performed with a BD Biosciences FACSCalibur or FACSCanto System using the CellQuest Professional or Diva software.

Assessment of the humoral immune response

Serum levels of IgG isotypes were determined by sandwich ELISA using goat anti-mouse IgG Ab as capture Ab and HRP-conjugated Abs for detection of IgG1, IgG2a, IgG2b, and IgG3 isotypes (Dianova). Serial dilutions of serum samples are indicated in Fig. 5*B*. Abs against dsDNA were detected by indirect ELISA at the indicated dilutions on plates coated with calf thymus DNA (5 μg/ml; Sigma-Aldrich) and alkaline phosphatase-conjugated goat anti-mouse polyvalent Ig Ab (Sigma-Aldrich). Serum from MRL/*lpr* mice was used in 1/100–1/12,500 dilution as positive control in autoantibody assays.

Statistical analysis

Results are expressed as individual data points. The horizontal line represents the mean. Differences between individual experimental groups were compared by Kruskal-Wallis test with post hoc analysis by Mann-Whitney *U* test. Those experiments that did not yield enough independent data for statistical analysis due to the experimental setup were repeated at least three times.

Results

*Generation and characterization of MRL/*lpr *CXCR3$^{-/-}$ mice*

The targeting strategy outlined in Fig. 1*A* was used to generate CXCR3$^{-/-}$ mice with a complete deletion of exon 2 of the CXCR3 gene (22). Using PCR analysis, all animals were genotyped for the *fas* mutation and CXCR3 status, as described in *Materials and Methods* (Fig. 1*B*). To confirm the absence of the CXCR3 protein, FACS analyses were performed, which showed CXCR3 expression on ~25% of CD3$^+$ T cells from spleens of MRL/*lpr* mice, whereas CD3$^+$ T cells from MRL/*lpr* CXCR3$^{-/-}$ mice were negative (Fig. 1*C*).

To assess the H-2 class I and II haplotypes, which differ between MRL and C57BL/6 mice, FACS analyses were performed. These showed that leukocytes from peripheral blood of MRL/*lpr* wild-type and MRL/*lpr* CXCR3$^{-/-}$ mice solemnly express the MRL

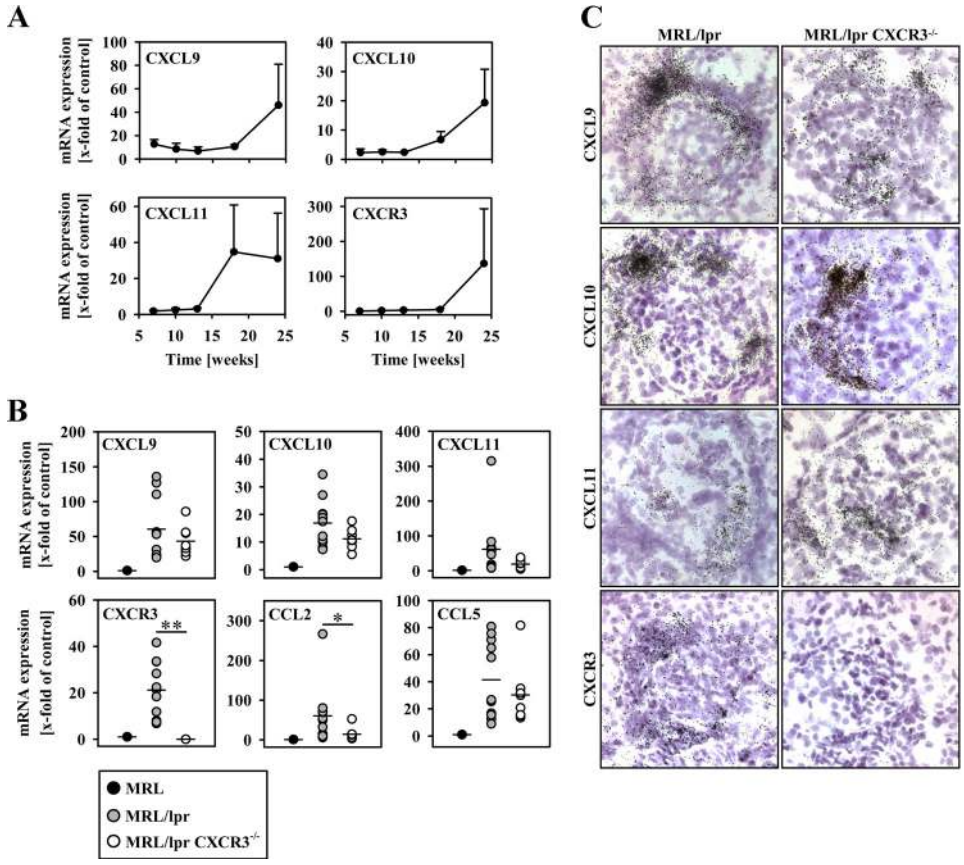

FIGURE 2. Renal expression of CXCR3 ligands. *A*, Time-dependent mRNA expression of CXCR3 and its three ligands in MRL/*lpr* mice as compared with MRL controls. *B*, At 20 wk of age, mRNA expression levels of CXCR3 and its ligands as well as CCL2 and CCL5 were significantly up-regulated in MRL/*lpr* mice ($n = 11$) as compared with MRL controls ($n = 6$). Chemokine expression levels were slightly lower in MRL/*lpr* CXCR3$^{-/-}$ animals ($n = 8$), but only CCL2 reached statistical significance. No CXCR3 mRNA expression was found in knockout mice. Symbols represent individual data points, and vertical lines represent means (*, $p < 0.05$ and **, $p < 0.01$). *C*, In situ hybridization showed expression of CXCR3 and its ligands in the glomerular and periglomerular compartments. No differences were seen in the distributional pattern of the chemokines between MRL/*lpr* wild-type and CXCR3$^{-/-}$ mice. No CXCR3 mRNA was detected in knockout mice.

characteristic κ allele, whereas no expression of the C57BL/6 characteristic β allele could be detected (supplemental Fig. 1).[5] Furthermore, SNP analysis of the complete autosome showed >99% MRL/*lpr* background in CXCR3 intact as well as CXCR3 knockout MRL/*lpr* littermates with no residual C57BL/6 or 129sv/PAS genomic DNA background. Screening of the X chromosome showed complete MRL/*lpr* background with the exception of the regions surrounding the CXCR3 gene. Here MRL/*lpr* CXCR3 knockout mice still have fragments of the C57BL/6 background (supplemental Table I). MRL/*lpr* CXCR3$^{-/-}$ mice were viable, fertile, and showed no developmental defects in comparison with MRL/*lpr* mice (data not shown).

*Chemokine and chemokine receptor expression in MRL/*lpr *nephritis*

Real-time quantitative PCR was performed to compare intrarenal expression of CXCR3 and its ligands Mig/CXCL9, IP10/CXCL10, and ITAC/CXCL11 between MRL/*lpr* mice and nonnephritic MRL controls at five different time points (Fig. 2*A*). mRNA expression of the receptor and all three ligands was already increased at 8 wk of age and continued to increase until the last time point analyzed, i.e., at 25 wk of age.

Analysis of chemokine mRNA from kidneys of 20-wk-old nephritic mice showed a lower, but statistically insignificant expression level of all three CXCR3 ligands in knockout animals as compared with wild-type mice. Analysis of monocyte-attracting chemokines showed a significantly less pronounced increase in MCP1/CCL2 expression in CXCR3$^{-/-}$ animals, whereas expression of RANTES/CCL5 was similar in both types of mice (Fig. 2*B*).

To localize intrarenal chemokine and chemokine receptor expression, we performed in situ hybridization. Strong Mig/CXCL9, IP10/CXCL10, and ITAC/CXCL11 expression was found in interstitial inflammatory infiltrates, inside glomeruli, and in the periglomerular area. No difference was seen in the expression pattern between MRL/*lpr* and MRL/*lpr* CXCR3$^{-/-}$ mice. CXCR3 mRNA was expressed in an overlapping pattern with the three chemokine ligands in MRL/*lpr* mice, whereas CXCR3$^{-/-}$ mice showed no staining (Fig. 2*C*).

Renal T cell and monocyte recruitment

To investigate renal T cell infiltration, immunohistochemical staining for the pan T cell marker CD3 was performed. For analysis of compartment-specific monocyte infiltration, two different immunohistochemical staining methods (MAC-2 and F4/80) were used, because MAC-2 is suitable for monocyte detection in glomeruli, but not in the tubulointerstitium. In contrast, F4/80 is more sensitive for the detection of interstitial monocytes, but less specific for monocytes in the glomeruli. Representative staining patterns are shown in Fig. 3*A*.

Quantification of CD3$^+$ cells revealed a significant increase in glomerular T cells in MRL/*lpr* wild-type mice when compared with MRL controls of the same age. MRL/*lpr* CXCR3$^{-/-}$ mice, however, showed significantly fewer glomerular T cell infiltrates when compared with MRL/*lpr* wild-type mice. Unlike in MRL controls, tubulointerstitial T cell infiltration was also highly increased in MRL/*lpr* wild-type mice. As in the glomeruli, interstitial T cell infiltration was significantly reduced in MRL/*lpr* CXCR3$^{-/-}$ mice when compared with MRL/*lpr* wild-type mice (Fig. 3*B*).

[5] The online version of this article contains supplemental material.

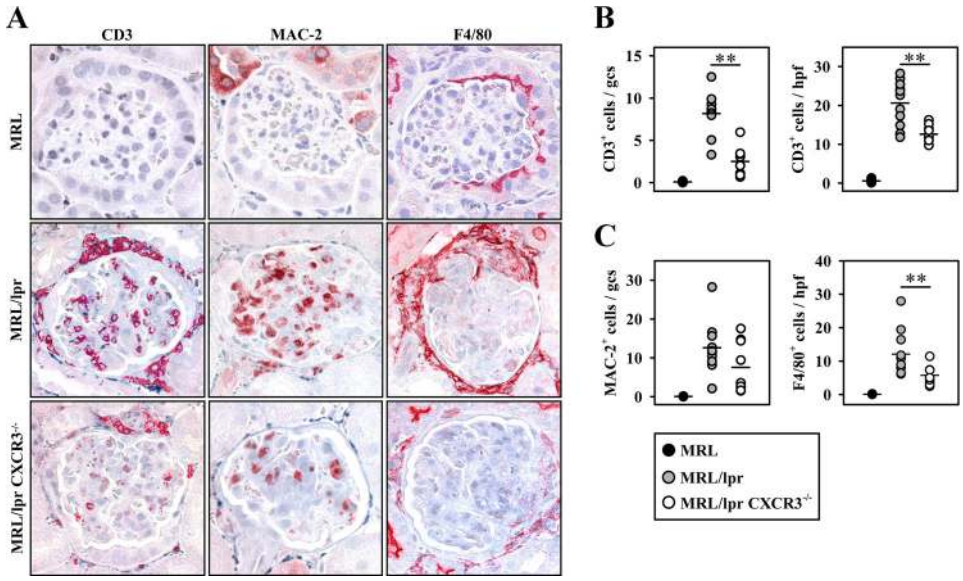

FIGURE 3. Renal T cell and monocyte recruitment. *A*, Representative immunohistochemical staining for $CD3^+$ T cells, $F4/80^+$ interstitial, and $MAC\text{-}2^+$ glomerular monocytes/macrophages in MRL controls, MRL/*lpr* wild-type, and MRL/*lpr* $CXCR3^{-/-}$ mice (original magnification: ×400). *B*, Quantification of glomerular and interstitial T cells revealed a significant reduction in MRL/*lpr* $CXCR3^{-/-}$ animals ($n = 9$) as compared with MRL/*lpr* wild-type mice ($n = 11$). Almost no infiltrating T cells were found in MRL controls ($n = 5$). *C*, Quantification of glomerular $MAC\text{-}2^+$ monocytes/macrophages and interstitial $F4/80^+$ monocytes/macrophages in MRL/*lpr* $CXCR3^{-/-}$ animals ($n = 9$) as compared with MRL/*lpr* wild-type mice ($n = 11$). Very few infiltrating monocytes/macrophages were found in MRL controls ($n = 5$). Symbols represent individual data points, and vertical lines represent means (**, $p < 0.01$).

In comparison with control mice, both MRL/*lpr* wild-type and MRL/*lpr* $CXCR3^{-/-}$ mice showed a significant increase in tubulointerstitial and glomerular monocyte recruitment. Although there was a decrease in infiltrating glomerular monocytes in MRL/*lpr* $CXCR3^{-/-}$ mice when compared with MRL/*lpr* wild-type mice, the reduction was not statistically significant. In contrast, tubulointerstitial monocyte infiltration in MRL/*lpr* $CXCR3^{-/-}$ mice was significantly reduced as compared with MRL/*lpr* wild-type mice (Fig. 3*C*).

Assessment of renal histological injury

PAS staining of renal tissue at the time of sacrifice showed severe glomerular damage with crescent formation and capillary necrosis in MRL/*lpr* wild-type mice, as has previously been described for this model. Glomerular lesions in MRL/*lpr* $CXCR3^{-/-}$ mice, however, were significantly reduced (Fig. 4*A*). Electron microscopic examination confirmed the light microscopic findings. In MRL control mice, there was only mild segmental expansion of the mesangium, with few mesangial deposits. Glomerular basement membranes and podocytes appeared normal. MRL/*lpr* wild-type mice showed severe mesangial expansion with increased matrix deposition, increased cell numbers, activated mesangial cells, and electron-dense deposits. Capillary lumina frequently contained leukocytes. The glomerular basement membranes showed irregularities that included newly formed matrix and frequent subepithelial and few subendothelial deposits. Podocytes displayed extensive effacement of foot processes. MRL/*lpr* $CXCR3^{-/-}$ mice, in comparison, showed only mild expansion of the mesangium, but a similar amount of mesangial electron-dense deposits. Peripheral glomerular basement membranes and podocyte foot processes were mostly well preserved. There were no subepithelial or subendothelial deposits (Fig. 4*B*).

To quantify renal tissue damage, kidney sections from 20-wk-old MRL/*lpr* $CXCR3^{-/-}$, MRL/*lpr* wild-type, and healthy MRL control mice were evaluated for the presence of glomerular crescents and capillary necrosis. The frequency of crescents was significantly decreased in MRL/*lpr* $CXCR3^{-/-}$ mice compared with MRL/*lpr* wild-type animals. Furthermore, glomeruli of MRL/*lpr* $CXCR3^{-/-}$ mice showed a significantly lower frequency of capillary necrosis. MRL control mice did not show any crescents or capillary necrosis (Fig. 4*C*).

Assessment of functional renal impairment

Albuminuria normalized to urinary creatinine was assessed at 10, 15, and 20 wk of age. MRL/*lpr* wild-type mice showed a markedly increased albumin to creatinine ratio at 15 and 20 wk of age compared with MRL control mice. However, the albumin to creatinine ratio was dramatically reduced in MRL/*lpr* $CXCR3^{-/-}$ mice when compared with MRL/*lpr* wild-type mice at these time points (Fig. 4*D*). Furthermore, BUN levels were assessed at the time of sacrifice (20 wk of age). BUN levels of MRL/*lpr* wild-type mice were significantly higher than those of nonnephritic MRL controls. BUN levels in MRL/*lpr* $CXCR3^{-/-}$ mice tended to be lower than in MRL/*lpr* wild-type mice, but differences were not statistically significant (Fig. 4*E*).

Renal Th1 and Th17 immune responses

To assess the role of Th1 and Th17 immune responses in MRL/*lpr* nephritis and the effects of CXCR3 deficiency, we performed intracellular staining for the Th1 prototype cytokine IFN-γ and for IL-17, the characteristic Th17 cytokine. Analyses showed a slightly reduced percentage of IFN-γ-producing $CD3^+$ and $CD4^+$ T cells in kidneys of MRL/*lpr* $CXCR3^{-/-}$ mice as compared with their MRL/*lpr* wild-type counterparts. It is of note, however, that in comparison with MRL/*lpr* wild-type mice, the total number of infiltrating T cells was significantly reduced, which confirms our data from the previous immunohistochemical studies. Furthermore, a large number of $IL\text{-}17^+$ intrarenal T cells was seen in MRL/*lpr* wild-type mice, whereas these IL-17-producing T cells were almost completely absent in MRL/*lpr* $CXCR3^{-/-}$ mice (Fig. 5*A*). No significant numbers of IFN-γ- or IL-17-expressing T cells

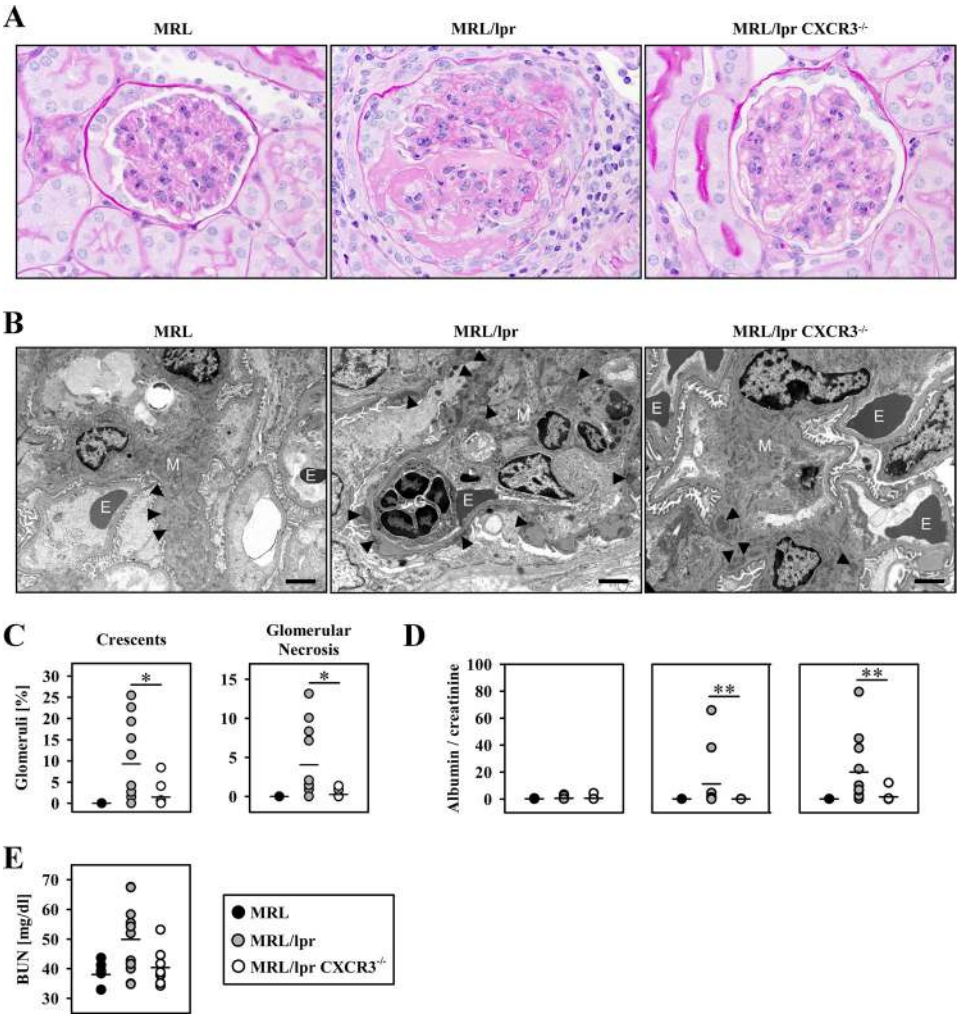

FIGURE 4. Renal tissue damage and impairment of renal function. *A*, Representative PAS staining of kidney sections at week 20 showed severe glomerular damage in MRL/*lpr* wild-type mice and less pronounced injury in MRL/*lpr* CXCR3$^{-/-}$ mice (original magnification: ×630). MRL controls showed no glomerular abnormalities. *B*, Representative electron microscopy of MRL control, MRL/*lpr* wild-type, and MRL/*lpr* CXCR3$^{-/-}$ mice (original magnification: ×4400). Arrowheads denote mesangial, subendothelial, and subepithelial deposits (E = erythrocyte, M = mesangium, G = granulocyte). Bar equals 2 μm. *C*, Quantification of glomerular damage revealed significantly less crescent formation and capillary necrosis in MRL/*lpr* CXCR3$^{-/-}$ mice ($n = 9$) as compared with their wild-type counterparts ($n = 11$). *D*, Albuminuria at 10, 15, and 20 wk of age in MRL controls ($n = 6$), MRL/*lpr* wild-type animals ($n = 11$), and MRL/*lpr* CXCR3$^{-/-}$ mice ($n = 8$). CXCR3$^{-/-}$ mice were almost completely protected from damage at 15 and 20 wk of age (**, $p < 0.01$). *E*, BUN levels at 20 wk of age were substantially, but not significantly ($p = 0.09$ NS), reduced in MRL/*lpr* CXCR3$^{-/-}$ mice ($n = 8$) as compared with nephritic wild-type mice ($n = 11$). Symbols represent individual data points, and vertical lines represent means.

were found in MRL control animals (data not shown). Interestingly, no double-positive IL-17- and IFN-γ-producing renal T cells were detectable, underscoring the dichotomy of these T cell subtypes (data not shown). To test whether the reduction in IFN-γ- and IL-17-producing T cells was due to impaired T cell trafficking or to a defect in generating Th1 or Th17 cells in CXCR3$^{-/-}$ mice, we analyzed spleens, renal lymph nodes, and the epithelium and lamina propria of the small intestine. The percentage of IFN-γ-producing T cells in spleens and lymph nodes of MRL/*lpr* wild-type and MRL/*lpr* CXCR3$^{-/-}$ animals, in contrast to the situation in inflamed kidneys, was comparable. As expected, the percentage of IL-17-expressing T cells was very low in secondary lymphoid organs of wild-type and CXCR3$^{-/-}$ mice (Fig. 5, *B* and *C*). To better characterize the Th17 response, we analyzed intraepithelial and lamina propria lymphocytes, because it is well known that IL-17-producing CD4$^+$ T cells are constitutively present in the gastrointestinal tract (30). Both intestinal T cell populations contained a significant number of IL-17-producing T cells in MRL/*lpr* wild-type mice. Interestingly, unlike in nephritic kidneys, the percentage of IL-17$^+$ T cells in both tissues of the small intestine was even higher in MRL/*lpr* CXCR3$^{-/-}$ mice (Fig. 5*D*). In contrast, the percentage of IFN-γ$^+$ T cells among these intestinal T cell populations was reduced in MRL/*lpr* CXCR3$^{-/-}$ mice compared with their wild-type littermates.

Characterization of renal and systemic CXCR3-positive cells

To further validate whether the general reduction of T cells, as well as the Th1 and Th17 subsets, observed in CXCR3 knockout mice was due to impaired trafficking of these cells, six-color FACS analyses (CXCR3, CD3, CD4, CD8, IFN-γ, and IL-17) of infiltrating renal cells and splenocytes were performed. Results showed that CXCR3 was predominantly expressed in both organs on CD4$^+$ Th cells, whereas most CD8$^+$ and double-negative (DN) T cells did not express this receptor (Fig. 6*A*).

Comparable results were seen with regard to IFN-γ-positive cells. More than half of renal IFN-γ-expressing CD4$^+$ T cells carried the CXCR3, whereas most IFN-γ-positive CD8$^+$ and DN T cells did not. CXCR3 was also found to be present on renal IL-17-expressing T cells. Approximately one-third of CD4$^+$ and CD8$^+$ T cells and one-half of DN IL-17-expressing T cells were CXCR3 positive (Fig. 6*B*). Numbers of CXCR3-positive IFN-γ-producing T cells in the spleen were smaller than in the kidney, but analysis of subtypes showed the same pattern (Fig. 6*C*). As expected, no significant IL-17 production was observed in splenocytes (data not shown).

Renal and systemic immune responses

To investigate whether CXCR3 deficiency induces alterations in the humoral immune response, we performed immunohistochemical staining for mouse IgG and complement C3 in kidneys of

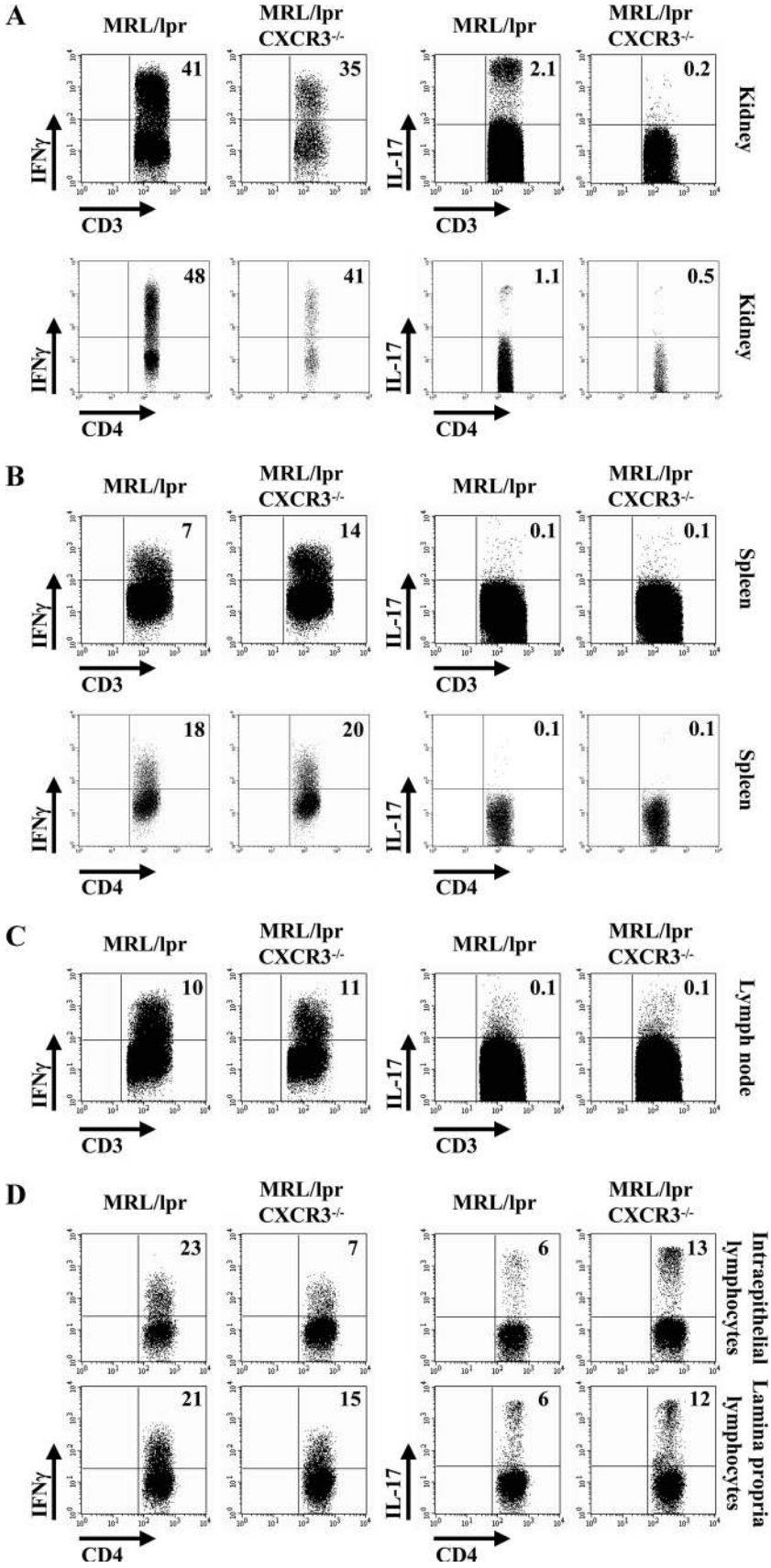

FIGURE 5. Renal Th1 and Th17 immune responses. *A*, FACS analysis showed a reduced number of IFN-γ-producing $CD3^+$ and $CD4^+$ T cells in kidneys from MRL/*lpr* $CXCR3^{-/-}$ mice as compared with their wild-type counterparts. IL-17-producing T cells were clearly present in kidneys of MRL/*lpr* wild-type mice, whereas this population was almost completely absent in MRL/*lpr* $CXCR3^{-/-}$ animals. Spleens (*B*) and lymph nodes (*C*) of both MRL/*lpr* wild-type and $CXCR3^{-/-}$ animals showed a similar population of IFN-γ-producing T cells, whereas the frequency of IL-17-producing T cells was low. *D*, IFN-γ-producing $CD4^+$ T cells were reduced in intraepithelial and lamina propria lymphocytes of MRL/*lpr* $CXCR3^{-/-}$ mice. The numbers of IL-17-producing T cells in both leukocyte populations were increased in MRL/*lpr* $CXCR3^{-/-}$ animals as compared with their wild-type counterparts. Plots are representative of three independent experiments.

20-wk-old MRL control, MRL/*lpr* wild-type, and MRL/*lpr* $CXCR3^{-/-}$ mice. As shown in Fig. 5*A*, no difference was found in the degree of glomerular IgG deposition between MRL/*lpr* wild-type and MRL/*lpr* $CXCR3^{-/-}$ mice. Further analyses of IgG subclasses did not show any difference in Ab deposition of IgG1, IgG2a, IgG2b, or IgG3 either (supplemental Fig. 2). C3 deposition,

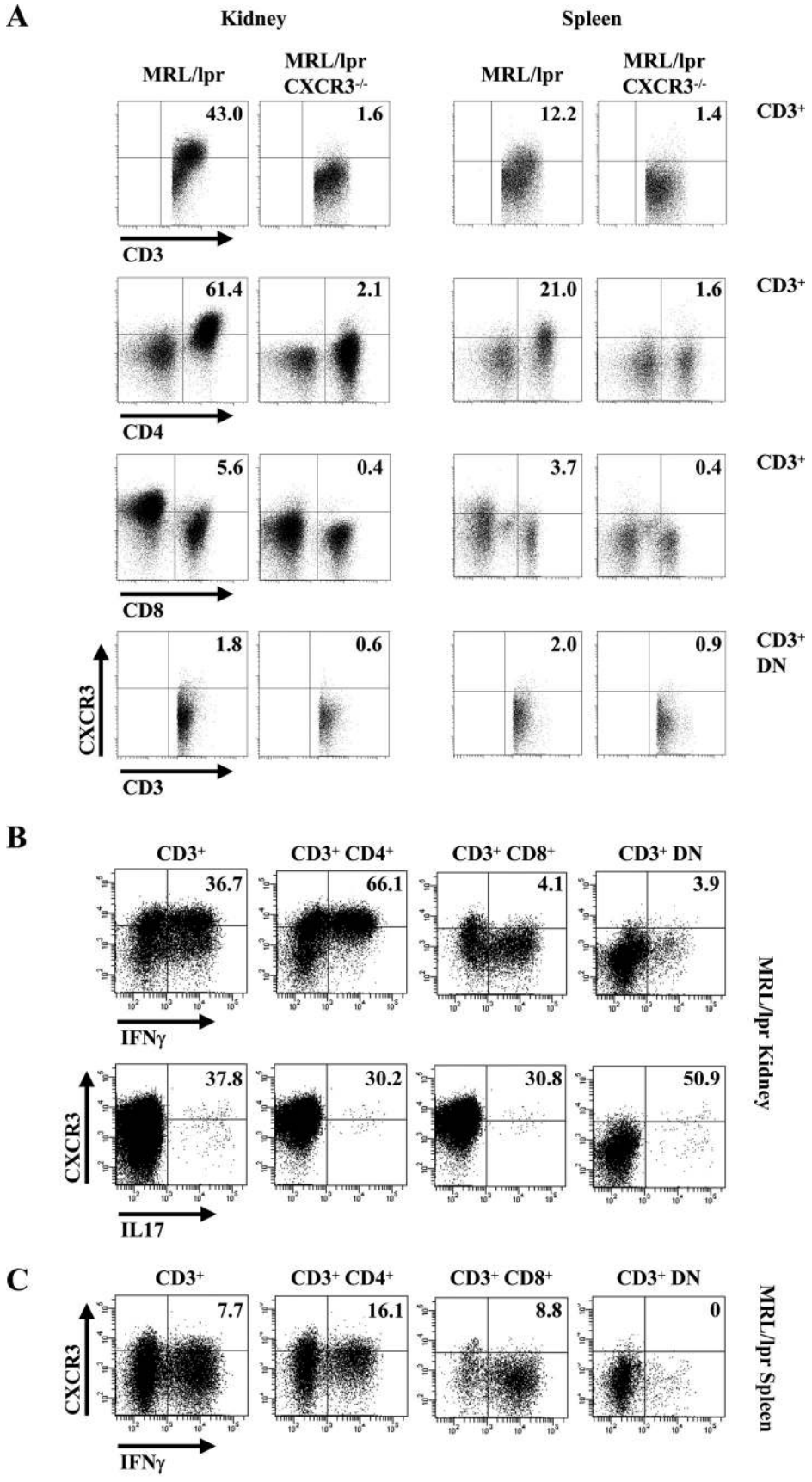

FIGURE 6. Characterization of renal and systemic CXCR3-positive cells. *A*, FACS analysis showed that ~40% of renal CD3-positive T cells express CXCR3. Analysis of T cell subpopulations showed that ~60% of CD4-positive Th cells are CXCR3 positive, whereas most $CD8^+$ and DN T cells are largely CXCR3 negative. In the spleen, numbers of CXCR3-positive cells are generally smaller (~10% of $CD3^+$ T cells). Approximately 20% of $CD4^+$ T cells express CXCR3, whereas $CD8^+$ and DN subsets are negative. No CXCR3 expression was found in $CXCR3^{-/-}$ animals. Plots in the *top three rows* are pregated on CD3, and the *bottom row* is pregated on CD3-positive and CD4/CD8 DN cells. *B*, Approximately 65% of renal IFN-γ-expressing $CD4^+$ T cells carry the CXCR3, whereas most IFN-γ-positive $CD8^+$ and DN T cells do not. CXCR3 was also found to be present on renal IL-17-expressing T cells. Approximately 30% of $CD4^+$ and $CD8^+$ T cells and 50% of DN IL-17-expressing T cells were CXCR3 positive. *C*, Numbers of CXCR3-positive IFN-γ-producing T cells in the spleen are smaller, but analysis of subtypes shows the same pattern as in the kidney. No significant IL-17 production was observed in splenocytes. Plots in *A–C* are representative of three independent experiments.

however, was slightly reduced in MRL/*lpr* $CXCR3^{-/-}$ mice when compared with their wild-type counterparts. MRL control mice did not show relevant IgG or C3 deposition (Fig. 7*A*).

To assess the systemic humoral immune response, we analyzed the isotype pattern of IgG Abs in the serum of nephritic mice using ELISA. Quantification of IgG isotypes revealed no bias for either

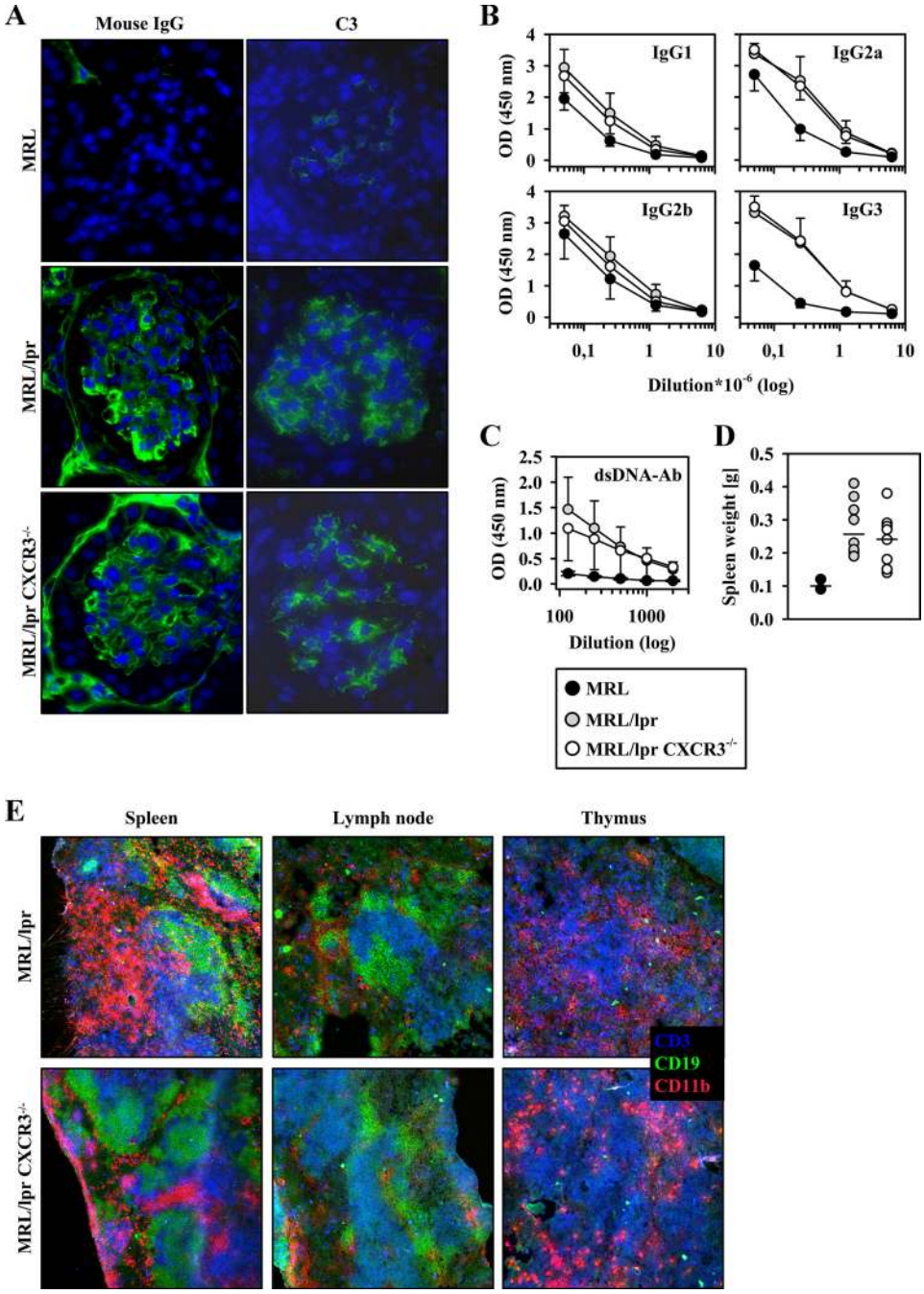

FIGURE 7. Renal and systemic immune responses. *A*, Immunohistochemical staining for mouse IgG showed identical deposition in both MRL/*lpr* wild-type and CXCR3$^{-/-}$ animals, whereas C3 deposition was slightly reduced. MRL control kidneys did not contain relevant amounts of IgG or C3 (original magnification: ×400). *B*, Quantification of IgG subclasses did not reveal any differences between MRL/*lpr* wild-type and CXCR3$^{-/-}$ animals. *C*, Analysis of dsDNA Abs showed significant up-regulation in nephritic animals as compared with MRL controls ($n = 6$). The levels in MRL/*lpr* wild type ($n = 12$) were comparable to those detected in CXCR3$^{-/-}$ ($n = 11$) animals. *D*, Comparison of spleen weight demonstrated a similar degree of lymphoproliferation in both MRL/*lpr* wild-type ($n = 11$) and CXCR3$^{-/-}$ mice ($n = 8$). Spleen weights of MRL control animals ($n = 3$) were significantly lower than in the two other groups. *E*, Triple immunostaining of lymphatic organs for the T cell marker CD3 (blue), the B cell marker CD19 (green), and the monocyte marker CD11b (red) showed no difference between MRL/*lpr* wild-type and CXCR3$^{-/-}$ animals. The microarchitecture with separate T cell, B cell, and monocyte zones was completely preserved (original magnification: 100-fold). Symbols represent individual data points, and vertical lines represent means.

Th1 (IgG2a, IgG3)- or Th2 (IgG1)-type Ab production in MRL/*lpr* CXCR3$^{-/-}$ mice compared with MRL/*lpr* wild-type mice. Abs of the IgG2b isotype were also present in comparable amounts in MRL/*lpr* CXCR3$^{-/-}$ mice and MRL/*lpr* wild-type mice (Fig. 7*B*). Abs against dsDNA typically present in SLE were significantly up-regulated in MRL/*lpr* wild-type animals compared with MRL control mice. However, the titers in MRL/*lpr* wild-type animals were comparable to those of MRL/*lpr* CXCR3$^{-/-}$ mice (Fig. 7*C*).

Because MRL/*lpr* mice spontaneously develop a lymphoproliferative disease with marked enlargement of secondary lymphoid organs, we measured the spleen weight. In comparison with MRL control mice, both MRL/*lpr* wild-type and MRL/*lpr* CXCR3$^{-/-}$ mice showed a similar enlargement of the spleen (Fig. 7*D*). To examine whether CXCR3 deficiency results in a general defect during ontogenesis of the immune system, we analyzed the architecture of secondary and primary lymphatic organs at the time of sacrifice. As can be seen in Fig. 7*E*, the spleen and lymph node architecture was unaltered in CXCR3$^{-/-}$ MRL/*lpr* mice, and showed clear segregation of CD3$^+$ T cell, CD19$^+$ B cell, and CD11b$^+$ monocyte/macrophage regions. The vast majority of cells in the thymus of both wild-type and CXCR3$^{-/-}$ mice were CD3$^+$ T cells (thymocytes), with a smaller population of CD11b$^+$ monocytes/macrophages.

Detection of CXCR3 and IP-10/CXCL10 in human lupus nephritis

To investigate whether the chemokine receptor CXCR3 might also be involved in renal T cell trafficking in human lupus nephritis, we performed serial and double staining for CD4 and CXCR3 in renal biopsies from patients with World Health Organization type IV lupus nephritis. Representative stainings are shown in Fig. 8, *A* and *B*, demonstrating that a large portion of infiltrating CD4$^+$ T cells

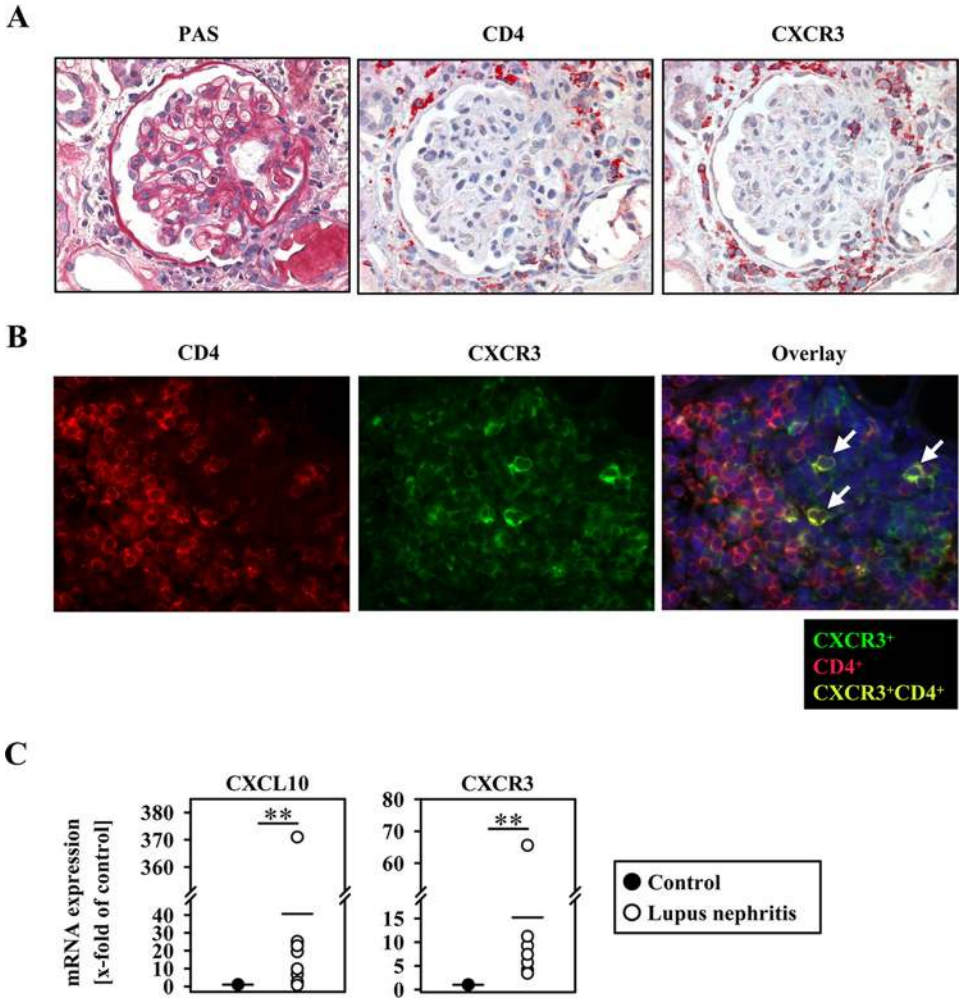

FIGURE 8. CXCR3 in human lupus nephritis. *A*, PAS, CD4, and CXCR3 staining of a glomerulus from a patient with World Health Organization type IV lupus nephritis. Serial staining shows that most infiltrating $CD4^+$ T cells coexpress the chemokine receptor CXCR3 (original magnification: ×400). *B*, Immunofluorescence double staining confirmed the presence of CXCR3 on infiltrating $CD4^+$ T cells in human World Health Organization type IV lupus nephritis. Examples of double-positive cells are indicated by arrows (CXCR3, green; CD4, red; double positive, yellow; nuclei, blue; original magnification: ×630). *C*, Quantification of mRNA from biopsies of 12 patients with lupus nephritis and five controls shows up-regulation of both CXCR3 and its ligand IP10/CXCL10 in lupus nephritis. Symbols represent individual data points, and vertical lines represent means (**, $p < 0.01$).

expresses the CXCR3 on their surface. No significant CXCR3 positivity was seen on resident kidney cells.

To analyze intrarenal expression of CXCR3 and its ligand IP10/CXCL10, RNA was isolated from renal biopsy specimens obtained from nine lupus patients with World Health Organization type IV and three patients with World Health Organization type III proliferative lupus nephritis. Renal biopsies from five patients without renal autoimmune disease served as controls. mRNA analysis revealed a significantly higher IP10/CXCL10 mRNA expression in the group of lupus patients compared with the healthy control group (Fig. 8*C*).

Discussion

In a wide range of human inflammatory diseases such as glomerulonephritis (31, 32), renal transplant rejection (25, 33), rheumatoid arthritis (34), and multiple sclerosis (35), the chemokine receptor CXCR3 has been localized to infiltrating effector T cells. The three CXCR3 ligands, Mig/CXCL9, IP-10/CXCL10, and ITAC/CXCL11, have been shown to be expressed in an overlapping pattern with CXCR3-bearing Th cells in these diseases, arguing for a decisive role in the recruitment of $CXCR3^+$ cells (25, 31, 34, 35). Data from experimental models further support the functional importance of the CXCR3 receptor in T cell trafficking. Involvement of CXCR3 was reported in murine models of heart allograft rejection (36), autoimmune type 1 diabetes mellitus (37), and acute renal ischemic injury (38, 39). $CXCR3^{-/-}$ mice were largely protected from organ damage in these immunologically mediated diseases.

Beneficial effects have also been shown in two models of acute glomerulonephritis. Using a rat model of renal endothelial microvascular injury (24), our group was able to demonstrate that Ab neutralization of the CXCR3 ligand IP10/CXCL10 had beneficial effects. Moreover, we recently showed amelioration of renal disease in $CXCR3^{-/-}$ mice with nephrotoxic serum nephritis (NTN) (22). These observations have meanwhile been confirmed by a study conducted by another group that shows improved renal outcome in mice deficient in the CXCR3 or its ligand Mig/CXCL9 in NTN. Surprisingly, however, IP10/CXCL10 deficiency did not alter renal pathology (40). There is still a lack of evidence to support a protective role of interference with the CXCR3 receptor-ligand axis in chronic renal autoimmune disease, such as the lupus nephritis of MRL/*lpr* mice. As in NTN, IP10/CXCL10 deficiency did not lead to improvement of the clinical course of glomerulonephritis in this murine model of human lupus nephritis (40). The influence of CXCR3 deficiency has not been studied to date.

The beneficial effects of CXCR3 deficiency in glomerulonephritis have generally been attributed to impaired trafficking of Th1-polarized T cells to the kidney. However, no definite evidence has yet been found that the number of intrarenal T cells producing the Th1 prototype cytokine IFN-γ is reduced in $CXCR3^{-/-}$ mice. Furthermore, CXCR3 has recently been found to be also expressed on the Th17 cell population (19, 20). There are only sparse data on the role of the Th17 response in glomerulonephritis and no data at all on the effect of CXCR3 deficiency on Th17 cell trafficking. In this study, we show for the first time that CXCR3 deficiency improves renal outcome in the MRL/*lpr* model of lupus nephritis, not only by reducing the number of renal Th1 cells, but also by almost completely abolishing Th17 cell infiltration.

In agreement with published studies (40, 41), renal mRNA expression of all three CXCR3 ligands, Mig/CXCL9, IP-10/CXCL10, and ITAC/CXCL11, as well as CXCR3 mRNA, increased with progression of nephritis in MRL/*lpr* animals from 10 wk of age. At the time of sacrifice (20 wk of age), intrarenal chemokine levels of all CXCR3 ligands were slightly reduced in MRL/*lpr* CXCR3$^{-/-}$ mice. By contrast, MCP-1/CCL2 expression was significantly less enhanced in MRL/*lpr* CXCR3$^{-/-}$ mice. As shown by in situ hybridization, all three CXCR3 ligands were abundantly expressed inside inflamed glomeruli and in the periglomerular area. No significant difference was found in the distribution pattern between wild-type and knockout mice.

Despite similar intrarenal expression of the CXCR3 ligands, the total numbers of infiltrating T cells were significantly reduced inside the glomeruli and in the tubulointerstitium of CXCR3$^{-/-}$ mice. The number of tubulointerstitial monocytes/macrophages was also lower in CXCR3$^{-/-}$ mice, which may be secondary to substantially reduced renal expression of the monocyte-attracting chemokine MCP-1/CCL2. Because the MCP-1/CCL2 production by resident renal cells is stimulated by IL-17 (11), reduced expression might be a result of impaired renal Th17 cell infiltration. We cannot exclude, however, that CXCR3 expression on activated monocytes also contributes to the trafficking of this pathogenic cell population into the nephritic kidney, as was recently reported (40).

In accordance with reduced T cell and monocyte infiltration, renal tissue damage was substantially less pronounced in CXCR3$^{-/-}$ mice. Glomerular crescent formation and capillary necrosis were significantly reduced in CXCR3$^{-/-}$ mice as compared with their wild-type counterparts. Analysis by electron microscopy confirmed these data. Amelioration of the renal morphological damage led to direct improvement of renal function. In CXCR3$^{-/-}$ mice, albuminuria was substantially decreased and the BUN level tended to be lower.

To test the hypothesis that CXCR3 deficiency interferes with trafficking of Th1 and maybe also Th17 cells into the kidney, we performed FACS analyses of isolated renal leukocytes. CXCR3 expression on renal infiltrating cells was found predominantly on the CD4-positive Th cell subset. Approximately 60% of IFN-γ-producing Th1 cells were positive for CXCR3. Interestingly, we also found that approximately one-third of infiltrating IL-17-producing Th17 cells expressed high levels of CXCR3 on their surface. In agreement with these observations and our immunohistochemical studies, significantly reduced total numbers of intrarenal T cells, IFN-γ-secreting Th1, and IL-17-producing Th17 cells were found. However, the relative contribution of IFN-γ-secreting renal T cells to the total number of T cells was only slightly reduced. This might be due to alternative mechanisms of Th1 cell migration into the inflamed kidney, possibly via the chemokine receptors CCR5 and CXCR6, which are also known to be expressed on Th1-polarized cells (42). Alternatively, CXCR3 is likely to be involved in the trafficking of non-IFN-γ-producing T cells because we could show that a significant number of IFN-γ-negative cells also express CXCR3. In this case, one could hypothesize that similarly impaired migration of these cells restores the balance between infiltrating IFN-γ-positive and IFN-γ-negative cells. Th17 cells are one of the candidate cell populations in this process. Intrarenal T cells with high expression of the Th17-defining cytokine IL-17 were clearly present in nephritic wild-type mice. Strikingly, this population of highly pathogenic T effector cells was completely absent in CXCR3$^{-/-}$ animals. Because only about one-third of Th17 cells express CXCR3, other yet to be defined mechanisms probably contribute to this observation. It is likely that reduced recruitment of CXCR3-positive cells leads to less tissue damage and inflammation, which in turn reduces influx of further immune cells, including Th17 cells, independent of their CXCR3 expression.

To investigate whether a reduction in intrarenal IFN-γ- and IL-17-producing T cells might be due to an impaired cellular immune response in CXCR3$^{-/-}$ mice, we analyzed spleens and renal lymph nodes. In CXCR3$^{-/-}$ MRL/*lpr* mice, the total number and percentage of IFN-γ-producing T cells in these tissues were even slightly increased, showing their general ability to mount a physiological Th1 response. In accordance with published data (30), no relevant IL-17 production was found in either lymph nodes or spleens. We therefore analyzed two intestinal lymphocyte populations in which Th17 cells are constitutively present (30). FACS analyses showed a higher number and frequency of IL-17-producing T cells in lamina propria as well as in intraepithelial lymphocytes in CXCR3$^{-/-}$ mice, whereas the Th17 population in MRL/*lpr* wild-type animals was identical with that found in healthy control mice. These data demonstrate that a reduction in IL-17-producing T cells inside inflamed kidneys is not due to a general defect in the differentiation of Th17 cells, but rather argues for impaired trafficking of these cells in CXCR3$^{-/-}$ mice. The fact that systemic Th1 and Th17 immune responses are intact in CXCR3$^{-/-}$ animals highlights the potential use of CXCR3 blockade as therapeutic strategy in inflammatory kidney diseases. In contrast, neutralization of the shared p40 subunit of IL-12 and IL-23, the only other molecule known to simultaneously interfere with pathologic Th1 and Th17 responses, results in general immune defects, and is therefore likely to cause significant unwanted side effects.

Because CXCR3 deficiency might have effects on the humoral immune response (40), we evaluated glomerular and systemic IgG levels as well as glomerular complement deposition. By immunohistochemistry, no relevant difference was seen between MRL/*lpr* CXCR3$^{-/-}$ and wild-type mice with respect to glomerular binding of IgG and its subtypes. Deposition of complement C3 appeared slightly reduced in CXCR3$^{-/-}$ animals. Although the quantity of immune complexes was similar between the groups, electron microscopy revealed a differential pattern of deposition. The majority of Ig deposition in both strains of mice located to the mesangial area. However, subepithelial and subendothelial deposits, which are characteristic of more aggressive forms of lupus nephritis, were regularly present in the MRL/*lpr* wild-type mice and greatly reduced in CXCR3 knockout animals.

Analysis of systemic dsDNA Abs and IgG1, IgG2a, IgG2b, and IgG3 showed similar levels in both groups of animals. Amelioration of renal disease in CXCR3$^{-/-}$ MRL/*lpr* mice therefore seems to be more a result of an impaired cellular, rather than an impaired humoral immune response.

To assess possible general defects in the ontogenesis of the immune system in CXCR3$^{-/-}$ mice, we examined primary and secondary lymphatic organs. Spleens of both CXCR3 wild-type and CXCR3$^{-/-}$ mice showed the same degree of lymphoproliferation as assessed by measurement of the organ weights. Even more important, the tissue microarchitecture of spleen, lymph nodes, and thymus was unaltered in MRL/*lpr* CXCR3$^{-/-}$ mice as compared with their wild-type counterparts, arguing against general immune defects in CXCR3$^{-/-}$ animals.

To verify the genetic background of our experimental mice, screening of the complete genome was conducted. Importantly, analyses confirmed that the complete autosome, including all known lupus susceptibility loci as well as the H-2 region, was of the MRL/*lpr* genetic background. The X chromosome was also shown to be of MRL/*lpr* background, except fragments surrounding the CXCR3 locus, which remained of the C57BL/6 background. It is highly unlikely, however, that this small amount of residual non-MRL/*lpr* background results in specific impairment of cellular trafficking, whereas the renal humoral and the systemic humoral and cellular immune response is unchanged.

To investigate whether CXCR3 and its ligands are also involved in human lupus, we analyzed renal biopsies from patients with active lupus nephritis. In this study, we could demonstrate high intrarenal mRNA expression of CXCR3 and its ligand IP10/CXCL10 as well as CXCR3 bearing Th cells infiltrating the inflamed kidneys. These findings are in line with recently published data (43) and suggest that CXCR3-mediated renal T cell trafficking is not only important in murine, but also in human lupus nephritis.

Taken together, our data show for the first time that not only Th1, but also Th17 effector T cells mediate glomerulonephritis in MRL/*lpr* mice. Deficiency of the chemokine receptor CXCR3 leads to significant morphological and functional improvement of nephritic kidneys. These protective effects are mediated by interference with trafficking of both Th1 and Th17 cells into the inflamed kidneys. Moreover, we provide further evidence that CXCR3-bearing T cells are not only of importance in experimental, but also in human lupus nephritis. Therefore, CXCR3 blockade is a promising new strategy, especially in the light of the recently developed small molecular inhibitors.

Acknowledgments

We thank M. Reszka and U. Kneíssler for critical technical assistance.

Disclosures

The authors have no financial conflict of interest.

References

1. Ruiz-Irastorza, G., M. A. Khamashta, G. Castellino, and G. R. Hughes. 2001. Systemic lupus erythematosus. *Lancet* 357: 1027–1032.
2. Ward, M. M., E. Pyun, and S. Studenski. 1996. Mortality risks associated with specific clinical manifestations of systemic lupus erythematosus. *Arch. Intern. Med.* 156: 1337–1344.
3. Tipping, P. G., and S. R. Holdsworth. 2006. T cells in crescentic glomerulonephritis. *J. Am. Soc. Nephrol.* 17: 1253–1263.
4. Tipping, P. G., and A. R. Kitching. 2005. Glomerulonephritis, Th1 and Th2: what's new? *Clin. Exp. Immunol.* 142: 207–215.
5. Steinman, L. 2007. A brief history of T_H17, the first major revision in the T_H1/T_H2 hypothesis of T cell-mediated tissue damage. *Nat. Med.* 13: 139–145.
6. Cua, D. J., J. Sherlock, Y. Chen, C. A. Murphy, B. Joyce, B. Seymour, L. Lucian, W. To, S. Kwan, T. Churakova, et al. 2003. Interleukin-23 rather than interleukin-12 is the critical cytokine for autoimmune inflammation of the brain. *Nature* 421: 744–748.
7. Murphy, C. A., C. L. Langrish, Y. Chen, W. Blumenschein, T. McClanahan, R. A. Kastelein, J. D. Sedgwick, and D. J. Cua. 2003. Divergent pro and anti-inflammatory roles for IL-23 and IL-12 in joint autoimmune inflammation. *J. Exp. Med.* 198: 1951–1957.
8. Langrish, C. L., Y. Chen, W. M. Blumenschein, J. Mattson, B. Basham, J. D. Sedgwick, T. McClanahan, R. A. Kastelein, and D. J. Cua. 2005. IL-23 drives a pathogenic T cell population that induces autoimmune inflammation. *J. Exp. Med.* 201: 233–240.
9. Harrington, L. E., R. D. Hatton, P. R. Mangan, H. Turner, T. L. Murphy, K. M. Murphy, and C. T. Weaver. 2005. Interleukin 17-producing $CD4^+$ effector T cells develop via a lineage distinct from the T helper type 1 and 2 lineages. *Nat. Immunol.* 6: 1123–1132.
10. Kurts, C. 2008. Th17 cells: a third subset of $CD4^+$ T effector cells involved in organ-specific autoimmunity. *Nephrol. Dial. Transplant.* 23: 816–819.
11. Paust, H. J., J. E. Turner, O. M. Steinmetz, A. Peters, F. Heymann, C. Holscher, G. Wolf, C. Kurts, H. W. Mittrucker, R. A. Stahl, and U. Panzer. 2009. The IL-23/Th17 axis contributes to renal injury in experimental glomerulonephritis. *J. Am. Soc. Nephrol.* 20: 969–979.
12. Ooi, J. D., R. K. Phoon, S. R. Holdsworth, and A. R. Kitching. 2009. IL-23, not IL-12, directs autoimmunity to the Goodpasture antigen. *J. Am. Soc. Nephrol.* 20: 980–989.
13. Charo, I. F., and R. M. Ransohoff. 2006. The many roles of chemokines and chemokine receptors in inflammation. *N. Engl. J. Med.* 354: 610–621.
14. Moser, B., M. Wolf, A. Walz, and P. Loetscher. 2004. Chemokines: multiple levels of leukocyte migration control. *Trends Immunol.* 25: 75–84.
15. Panzer, U., O. M. Steinmetz, R. A. Stahl, and G. Wolf. 2006. Kidney diseases and chemokines. *Curr. Drug Targets* 7: 65–80.
16. Kulkarni, O., and H. J. Anders. 2008. Chemokines in lupus nephritis. *Front. Biosci.* 13: 3312–3320.
17. Rovin, B. H. 2008. The chemokine network in systemic lupus erythematous nephritis. *Front. Biosci.* 13: 904–922.
18. Sallusto, F., and A. Lanzavecchia. 2000. Understanding dendritic cell and T-lymphocyte traffic through the analysis of chemokine receptor expression. *Immunol. Rev.* 177: 134–140.
19. Singh, S. P., H. H. Zhang, J. F. Foley, M. N. Hedrick, and J. M. Farber. 2008. Human T cells that are able to produce IL-17 express the chemokine receptor CCR6. *J. Immunol.* 180: 214–221.
20. Lim, H. W., J. Lee, P. Hillsamer, and C. H. Kim. 2008. Human Th17 cells share major trafficking receptors with both polarized effector T cells and $FOXP3^+$ regulatory T cells. *J. Immunol.* 180: 122–129.
21. Hirota, K., H. Yoshitomi, M. Hashimoto, S. Maeda, S. Teradaira, N. Sugimoto, T. Yamaguchi, T. Nomura, H. Ito, T. Nakamura, et al. 2007. Preferential recruitment of CCR6-expressing Th17 cells to inflamed joints via CCL20 in rheumatoid arthritis and its animal model. *J. Exp. Med.* 204: 2803–2812.
22. Panzer, U., O. M. Steinmetz, H. J. Paust, C. Meyer-Schwesinger, A. Peters, J. E. Turner, G. Zahner, F. Heymann, C. Kurts, H. Hopfer, et al. 2007. Chemokine receptor CXCR3 mediates T cell recruitment and tissue injury in nephrotoxic nephritis in mice. *J. Am. Soc. Nephrol.* 18: 2071–2084.
23. Panzer, U., F. Thaiss, G. Zahner, P. Barth, M. Reszka, R. R. Reinking, G. Wolf, U. Helmchen, and R. A. Stahl. 2001. Monocyte chemoattractant protein-1 and osteopontin differentially regulate monocytes recruitment in experimental glomerulonephritis. *Kidney Int.* 59: 1762–1769.
24. Panzer, U., O. M. Steinmetz, R. R. Reinking, T. N. Meyer, S. Fehr, A. Schneider, G. Zahner, G. Wolf, U. Helmchen, P. Schaerli, et al. 2006. Compartment-specific expression and function of the chemokine IP-10/CXCL10 in a model of renal endothelial microvascular injury. *J. Am. Soc. Nephrol.* 17: 454–464.
25. Panzer, U., R. R. Reinking, O. M. Steinmetz, G. Zahner, U. Sudbeck, S. Fehr, B. Pfalzer, A. Schneider, F. Thaiss, M. Mack, et al. 2004. CXCR3 and CCR5 positive T-cell recruitment in acute human renal allograft rejection. *Transplantation* 78: 1341–1350.
26. Vielhauer, V., H. J. Anders, G. Perez de Lema, B. Luckow, D. Schlondorff, and M. Mack. 2003. Phenotyping renal leukocyte subsets by four-color flow cytometry: characterization of chemokine receptor expression. *Nephron Exp. Nephrol.* 93: e63.
27. Kursar, M., U. E. Hopken, M. Koch, A. Kohler, M. Lipp, S. H. Kaufmann, and H. W. Mittrucker. 2005. Differential requirements for the chemokine receptor CCR7 in T cell activation during *Listeria monocytogenes* infection. *J. Exp. Med.* 201: 1447–1457.
28. Kursar, M., K. Bonhagen, A. Kohler, T. Kamradt, S. H. Kaufmann, and H. W. Mittrucker. 2002. Organ-specific $CD4^+$ T cell response during *Listeria monocytogenes* infection. *J. Immunol.* 168: 6382–6387.
29. Korn, T., J. Reddy, W. Gao, E. Bettelli, A. Awasthi, T. R. Petersen, B. T. Backstrom, R. A. Sobel, K. W. Wucherpfennig, T. B. Strom, et al. 2007. Myelin-specific regulatory T cells accumulate in the CNS but fail to control autoimmune inflammation. *Nat. Med.* 13: 423–431.
30. Niess, J. H., F. Leithauser, G. Adler, and J. Reimann. 2008. Commensal gut flora drives the expansion of proinflammatory CD4 T cells in the colonic lamina propria under normal and inflammatory conditions. *J. Immunol.* 180: 559–568.
31. Segerer, S., B. Banas, M. Wornle, H. Schmid, C. D. Cohen, M. Kretzler, M. Mack, E. Kiss, P. J. Nelson, D. Schlondorff, and H. J. Grone. 2004. CXCR3 is involved in tubulointerstitial injury in human glomerulonephritis. *Am. J. Pathol.* 164: 635–649.
32. Romagnani, P., C. Beltrame, F. Annunziato, L. Lasagni, M. Luconi, G. Galli, L. Cosmi, E. Maggi, M. Salvadori, C. Pupilli, and M. Serio. 1999. Role for interactions between IP-10/Mig and CXCR3 in proliferative glomerulonephritis. *J. Am. Soc. Nephrol.* 10: 2518–2526.
33. Akalin, E., S. Dikman, B. Murphy, J. S. Bromberg, and W. W. Hancock. 2003. Glomerular infiltration by $CXCR3^+$ $ICOS^+$ activated T cells in chronic allograft nephropathy with transplant glomerulopathy. *Am. J. Transplant.* 3: 1116–1120.
34. Qin, S., J. B. Rottman, P. Myers, N. Kassam, M. Weinblatt, M. Loetscher, A. E. Koch, B. Moser, and C. R. Mackay. 1998. The chemokine receptors CXCR3 and CCR5 mark subsets of T cells associated with certain inflammatory reactions. *J. Clin. Invest.* 101: 746–754.
35. Balashov, K. E., J. B. Rottman, H. L. Weiner, and W. W. Hancock. 1999. $CCR5^+$ and $CXCR3^+$ T cells are increased in multiple sclerosis and their ligands MIP-1α and IP-10 are expressed in demyelinating brain lesions. *Proc. Natl. Acad. Sci. USA* 96: 6873–6878.
36. Hancock, W. W., B. Lu, W. Gao, V. Csizmadia, K. Faia, J. A. King, S. T. Smiley, M. Ling, N. P. Gerard, and C. Gerard. 2000. Requirement of the chemokine receptor CXCR3 for acute allograft rejection. *J. Exp. Med.* 192: 1515–1520.
37. Frigerio, S., T. Junt, B. Lu, C. Gerard, U. Zumsteg, G. A. Hollander, and L. Piali. 2002. β cells are responsible for CXCR3-mediated T-cell infiltration in insulitis. *Nat. Med.* 8: 1414–1420.
38. Fiorina, P., M. J. Ansari, M. Jurewicz, M. Barry, V. Ricchiuti, R. N. Smith, S. Shea, T. K. Means, H. Auchincloss, Jr., A. D. Luster, et al. 2006. Role of CXC chemokine receptor 3 pathway in renal ischemic injury. *J. Am. Soc. Nephrol.* 17: 716–723.
39. Steinmetz, O. M., S. Sadaghiani, U. Panzer, C. Krebs, C. Meyer-Schwesinger, T. Streichert, S. Fehr, I. Hamming, H. van Goor, R. A. Stahl, and U. Wenzel. 2007. Antihypertensive therapy induces compartment-specific chemokine expression and a Th1 immune response in the clipped kidney of Goldblatt hypertensive rats. *Am. J. Physiol.* 292: F876–F887.
40. Menke, J., G. C. Zeller, E. Kikawada, T. K. Means, X. R. Huang, H. Y. Lan, B. Lu, J. Farber, A. D. Luster, and V. R. Kelley. 2008. CXCL9, but not CXCL10, promotes CXCR3-dependent immune-mediated kidney disease. *J. Am. Soc. Nephrol.* 19: 1177–1189.
41. Teramoto, K., N. Negoro, K. Kitamoto, T. Iwai, H. Iwao, M. Okamura, and K. Miura. 2008. Microarray analysis of glomerular gene expression in murine lupus nephritis. *J. Pharmacol. Sci.* 106: 56–67.
42. Rot, A., and U. H. von Andrian. 2004. Chemokines in innate and adaptive host defense: basic chemokinese grammar for immune cells. *Annu. Rev. Immunol.* 22: 891–928.
43. Enghard, P., J. Y. Humrich, B. Rudolph, S. Rosenberger, R. Biesen, A. Kuhn, R. Manz, F. Hiepe, A. Radbruch, G. R. Burmester, and G. Riemekasten. 2009. $CXCR3^+CD4^+$ T cells are enriched in inflamed kidneys and urine and provide a new biomarker for acute nephritis flares in systemic lupus erythematosus patients. *Arthritis Rheum.* 60: 199–206.